Fermi National Accelerator Laboratory

FERMILAB-Pub-94/349-A
October 1994

LARGE SCALE BARYON ISOCURVATURE INHOMOGENEITIES

Craig J. Copi,[1] Keith A. Olive,[2] and David N. Schramm[1,3]

[1] *The University of Chicago, Chicago, IL 60637-1433*

[2] *School of Physics & Astronomy*
University of Minnesota, Minneapolis, MN 55455

[3] *NASA/Fermilab Astrophysics Center*
Fermi National Accelerator Laboratory, Batavia, IL 60510-0500

ABSTRACT

Big bang nucleosynthesis constraints on baryon isocurvature perturbations are determined. A simple model ignoring the effects of the scale of the perturbations is first reviewed. This model is then extended to test the claim that large amplitude perturbations will collapse, forming compact objects and preventing their baryons from contributing to the observed baryon density. It is found that baryon isocurvature perturbations are constrained to provide only a slight increase in the density of baryons in the universe over the standard homogeneous model. In particular it is found that models which rely on power laws and the random phase approximation for the power spectrum are incompatible with big bang nucleosynthesis unless an *ad hoc*, small scale cutoff is included.

Submitted to *The Astrophysical Journal*

1 Introduction

Big bang nucleosynthesis (BBN) has produced well studied predictions of the light element abundances (Yang *et al.* 1984; Walker *et al.* 1991, hereafter WSSOK: Smith, Kawano, & Malaney 1993; Kernan & Krauss 1994; Copi, Schramm, & Turner 1994). These predictions restrict the total baryonic contribution to the critical density of the universe, Ω_B, to be $\Omega_B \lesssim 0.1$. There have been many attempts to get around this bound and to extend it to the theoretically preferred value $\Omega_0 = 1$. A notable class of such attempts is inhomogeneous BBN (for a review see Malaney & Mathews 1993). These studies of small scale inhomogeneities in the neutron to proton ratio including hydrodynamic effects, diffusion, extended networks, and multizone calculations turn out, however, to provide no appreciable increase on the bound to Ω_B set by standard BBN (Kurki-Suonio et al., 1990; Mathews et al., 1990; Terasawa & Sato, 1991; Thomas et al. 1994; Jedamzik, Fuller, & Mathews, 1994).

On another front, structure formation theories are being constrained by a rapidly growing body of observational data. From this the primeval isocurvature baryon (PIB) model has fared relatively well. The PIB model relies solely on baryons to make up the matter in the universe and isocurvature perturbations to generate the structure (Peebles 1987a,b; Cen, Ostriker, & Peebles 1993). One short coming of this theory is that it requires $\Omega_0 = \Omega_B = 0.1-0.2$, above the upper bound on Ω_B from BBN. Independently, it has been suggested that non-linear isocurvature fluctuations may allow a larger contribution by baryons than allowed for in the standard, homogeneous case (Hogan 1978; Hogan 1993).

In this work we have looked at the effect of large scale isocurvature perturbations on nucleosynthesis. Our treatment follows that of Epstein & Petrosian (1975, hereafter EP) and Yang et al. (1984). In those efforts, it was assumed that the volume distribution for the nucleon abundance could be described by a gamma distribution in the baryon to photon ratio, η. The abundances of the light elements can then be used to constrain the parameters of the nucleon abundance distribution. Here we will update that analysis utilizing the most recent constraints available from the light elements including ^{7}Li. We will also consider additional forms for the nucleon abundance distribution to include the log normal (Barrows & Morgan 1983) and the gaussian (Sale & Mathews 1986) distributions. Furthermore we have extended the analysis to include a distribution of power on different scales to allow for dense regions to form compact objects and hence not contribute their light elements to the observed abundances.

For our model we assume the perturbations can be described by a power spectrum with random phases. We have no knowledge of the spatial distribution, $\eta(\boldsymbol{x})$, and instead specify the choice of the density probability distribution, $f(\eta)$. Recently Gnedin, Ostriker, & Rees (1994) have also considered the effects of baryon perturbations on nucleosynthesis. They chose a log-normal density distribution with two scales. We choose three different density distributions (including the log-normal distribution) defined on a single scale. We have not specifically chosen parameters to match those of the PIB model. Our results, where comparable, agree with theirs. Gnedin, Ostriker & Rees (1994) also approached the problem from the opposite direction; they assumed a form for $\eta(\boldsymbol{x})$ and derive a density distribution $f(\eta)$. They have found some models that can circumvent our bounds at the expense of assuming correlated phases.

An outline of the paper is as follows: in §2 we discuss the observational bounds on the light element abundances used in this paper, in particular, how they differ from the values found in WSSOK. In §3 we describe our model for the inhomogeneities. In §4 we present the results of our calculations.

2 Observational Limits

Observational measurements of the light element abundances play the crucial role of constraining the standard big bang nucleosynthesis model as well as models of nucleosynthesis which include inhomogeneities. The process of extracting abundances from the measurements, in particular primordial abundances, is a difficult task. An analysis of this process in the context of limits on BBN is given in WSSOK. The 95% confidence limit (2σ) primordial abundances quoted in WSSOK are

$$\begin{aligned} Y_P &= 0.23 \pm 0.01, \\ \mathrm{D/H} &\geq 1.8 \times 10^{-5}, \\ (\mathrm{D} + {}^3\mathrm{He})/\mathrm{H} &\leq 1.0 \times 10^{-4}, \\ {}^7\mathrm{Li/H} &= (1.2 \pm 0.2) \times 10^{-10}. \end{aligned} \tag{1}$$

Here Y_P is the ^{4}He mass fraction. These limits restrict the present value of η to $2.8 \leq \eta_{10} \leq 4.0$ ($\eta_{10} \equiv 10^{10}\eta$). In what follows we will use the WSSOK values with slight modifications to Y_P and ^{7}Li as discussed below.

It is noted in WSSOK that the upper limit on Y_P, $Y_P \leq 0.24$, may be uncertain by 0.005. More recently a number of high precision measurements of ^{4}He in extragalactic H II regions have been made (Pagel *et al.* 1992; Skillman *et al.* 1994a,b; Izotov *et al.* 1994). Olive and Steigman (1994) have performed a detailed statistical analysis of these new measurements and found the primordial helium value

$$Y_P = 0.232 \pm 0.003 \pm 0.005, \tag{2}$$

where the statistical error is listed first and the systematic error second. The 95% confidence range (including systematic errors) is

$$0.221 \leq Y_P \leq 0.243. \tag{3}$$

We will employ this range in our analysis.

The 95% confidence limit quoted by WSSOK for ^{7}Li/H consists solely of the statistical errors in the measurements. Recently Thorburn (1994) has made detailed measurements on a large number of metal poor dwarf stars. Her analysis employed a different model of stellar atmospheres than the one used to derive the data compiled in WSSOK. This model produces higher effective temperatures and hence higher lithium abundances. Her data yield a higher mean ^{7}Li abundance

$${}^7\mathrm{Li/H} = (1.8 \pm 0.1) \times 10^{-10} \tag{4}$$

where the quoted error is again only the statistical uncertainty in the mean. The difference between the ^{7}Li abundance given in (1) and (4) is a good estimate for the size of the systematic errors involved in making a determination of the the primordial ^{7}Li abundance. For this work we will consider both this new upper limit and the WSSOK upper limit.

In summary, we are using the primordial abundances of D and ^{3}He as found in WSSOK (1) and modifications of the WSSOK values of Y_P (3) and ^{7}Li (4) due to recent measurements with explicit consideration of systematic errors. The primordial abundance limits used throughout the rest of this work are

$$\begin{aligned} 0.221 \leq\ & Y_P \leq 0.243, \\ \mathrm{D/H} \geq\ & 1.8 \times 10^{-5}, \\ (\mathrm{D} + {}^3\mathrm{He})/\mathrm{H} \leq\ & 1.0 \times 10^{-4}, \\ {}^7\mathrm{Li/H} \leq\ & 1.4 \times 10^{-10} \quad \text{(WSSOK)}, \\ {}^7\mathrm{Li/H} \leq\ & 2.0 \times 10^{-10} \quad \text{(Thorburn 1994)}. \end{aligned} \tag{5}$$

The lithium bound is particularly important for constraining density fluctuations. In standard homogeneous BBN lithium must be nears its minimum value of $^7\mathrm{Li/H} \sim 10^{-10}$ in order to be concordant with D and D + ^{3}He. Obviously any density variation selects ^{7}Li values above the minimum, hence ^{7}Li tightly constrains the range of perturbations.

3 Model of Density Fluctuations

We begin with a simple model of inhomogeneities (EP). We assume that some unknown process generates a baryon to photon ratio $\eta(\boldsymbol{x})$ at each point in space in such a way that the fraction of regions with a given value η is governed by the distribution $f(\eta)$. We acknowledge our ignorance of the process that generates $\eta(\boldsymbol{x})$ by assuming (instead of deriving) the form of $f(\eta)$. Given $f(\eta)$ each region has a constant baryon to photon ratio η throughout nucleosynthesis. The regions undergo standard BBN, then mix producing the observed abundances of light elements. The distribution of these regions is described in our model by the function $f(\eta)$. Given the distribution $f(\eta)$ the average mass fraction of a light element is

$$\bar{X}_i = \int_0^\infty d\eta\, \eta f(\eta) X_i(\eta) \Big/ \bar{\eta}. \tag{6}$$

where $X_i(\eta)$ is the mass fraction of element i according to standard Big Bang nucleosynthesis in a region with a baryon to photon ratio of η. The average value of η for the universe is given by

$$\bar{\eta} = \int_0^\infty d\eta\, \eta f(\eta), \tag{7}$$

for $f(\eta)$ normalized,

$$\int_0^\infty d\eta\, \eta f(\eta) \equiv 1. \tag{8}$$

Shortcomings of this simple model include the assumption of equal power in perturbations on all scales and the allowance of extremely dense regions to contribute to the observed light element abundances today. It has been pointed out (Rees 1984) that high amplitude perturbations with a mass larger than the Jean's mass at the time of recombination will form gravitationally bound objects. These objects prevent the baryons in them from mixing with other baryons in the universe. Hence these overdense regions would not contribute to the observed abundances.

To determine a more realistic model, we consider isocurvature perturbations to the baryon to photon ratio. These perturbations are characterized by their power spectrum, $\langle|\delta_k|^2\rangle$. Given the power spectrum the average abundance is found by

$$\begin{aligned} \bar{X}_i &= \frac{\int \frac{d^3k}{(2\pi)^3} \langle|\delta_k|^2\rangle \int_0^{\eta_c(k)} d\eta\, \eta f(\eta) X_i(\eta)}{\int \frac{d^3k}{(2\pi)^3} \langle|\delta_k|^2\rangle \int_0^{\eta_c(k)} d\eta\, \eta f(\eta)} \\ &= \frac{\int_0^{k_{\max}} \frac{dk}{k} \Delta^2(k) \int_0^{\eta_c(k)} d\eta\, \eta f(\eta) X_i(\eta)}{\int \frac{dk}{k} \Delta^2(k) \int_0^{\eta_c(k)} d\eta\, \eta f(\eta)}. \end{aligned} \tag{9}$$

Here

$$\Delta^2(k) \equiv \frac{k^3}{2\pi^2} \langle|\delta_k|^2\rangle, \tag{10}$$

$\eta_c(k)$ is the cutoff in η based on the Jeans mass at recombination, and $k_{\max}$ is imposed to insure that the integrals converge. Since the Jeans mass at recombination, $M_J \propto \eta^{-1/2}$ (Hogan 1978; Hogan 1993) and the mass inside a scale k, $M_k \propto \eta/k^3$, the cutoff in η is

$$\eta_c(k) \propto k^2 \equiv \beta k^2, \tag{11}$$

where $\beta \approx 6 \times 10^{-14}$ for k in Mpc^{-1}. Using this relation and interchanging the order of integration in $\bar{X}_i$ (9) gives

$$\bar{X}_i = \frac{\int_0^{\eta_{\max}} d\eta\, \eta f(\eta) X_i(\eta) \int_{(\eta/\beta)^{1/2}}^{k_{\max}} \frac{dk}{k} \Delta^2(k)}{\int_0^{\eta_{\max}} d\eta\, \eta f(\eta) \int_{(\eta/\beta)^{1/2}}^{k_{\max}} \frac{dk}{k} \Delta^2(k)}, \tag{12}$$

where $\eta_{\max} \equiv \eta_c(k_{\max})$. In Eq. (12) our two assumptions are manifest. We have imposed an upper limit on $k_{\max}$ implying that there is no power in the perturbation spectrum on scales smaller than $\lambda_{\min} = 2\pi/k_{\max}$ and we have assumed that on sufficiently large scales, corresponding to $M_k > M_J$ or $k < \sqrt{\eta/\beta}$ gravitational collapse will prevent these regions from mixing the hence these regions to not contribute in an average element abundance. One should note however that the average value of η, $\bar{\eta}$ is not constrained by $\eta_{\max}$. The density distribution indeed includes regions with $\eta > \eta_{\max}$, though they do not contribute to the quantities $\bar{X}_i$. We will rewrite $k_{\max}$ in terms of $\eta_{\max}$ in the rest of this work.

4 Results

For $X_i(\eta)$ we have used the standard Kawano code (Kawano 1992) with $N_\nu = 3$, $\tau_n = 889$ sec and the correction $\Delta Y_P = +0.0006$ (Kernan 1993). We begin by reviewing previous work on the gamma and log normal distributions and provide an extended analysis of the gaussian distribution. Then we consider a model based on inclusion of the scale of the perturbations where the power spectrum is given by a power law.

4.1 Gamma Distribution

The gamma distribution (EP. Yang *et al.* 1984) is given by

$$f(\eta) = \eta^{a-1} e^{-a\eta/\bar{\eta}}. \tag{13}$$

For this distribution the variance δ^2, is

$$\delta^2 = \left(\frac{\delta\eta}{\bar{\eta}}\right)^2 = \frac{\langle \eta^2 \rangle - \bar{\eta}^2}{\bar{\eta}^2} = a^{-1}. \tag{14}$$

The results of varying δ^2 and $\bar{\eta}$ are shown in figure 1. We have required the averaged abundances to fit the observations (5). Figure 1 shows the abundance contours of the light elements as given by the limits in (5) and thus delineates the resulting parameter space that reproduces the correct abundances. In Yang et al. (1984) the parameters δ^2 and $\bar{\eta}$ were constrained to $\bar{\eta} \approx 3$ and $\delta^2 \lesssim 3$ without using the ^{7}Li bound and a weaker upper limit on ^{4}He of $Y_P < 0.25$. (For $\delta^2 < 1$, the upper bound on $\bar{\eta}$ is relaxed to the homogeneous upper bound.) Here, as one can see from the figure, the more restrictive ^{4}He bound combined with the bound from D + ^{3}He yet with the weaker bound from ^{7}Li (4) allows us to constrain $2.8 \lesssim \bar{\eta}_{10} \lesssim 3.6$. Including the WSSOK ^{7}Li bound this range is further constrained to $2.8 \lesssim \bar{\eta}_{10} \lesssim 3.3$. These results are summarized in table 1.

4.2 Log-Normal Distribution

The log-normal distribution (Barrow & Morgan 1983) is given by

$$f(\eta) = \frac{1}{\eta} \exp\left(-\frac{(\ln\eta - \mu)^2}{2\sigma^2}\right) \tag{15}$$

For this distribution

$$\bar{\eta} = e^{\mu+\sigma^2/2}. \tag{16}$$

The results of our search of parameter space are shown in figure 2. Using the weaker ^{7}Li bound (4) then $\bar{\eta}_{10} \lesssim 3.6$ is allowed. This result is similar to that given by Barrow and Morgan (1983), though we are using more restrictive bounds on D + ^{3}He and ^{4}He. If we include the WSSOK ^{7}Li bound we are restricted to $\bar{\eta}_{10} \lesssim 3.2$. These results are also included in table 1.

4.3 Gaussian Distribution

The gaussian distribution we consider is given by

$$f(\eta) = \exp\left(-\frac{(\eta-\mu)^2}{2\sigma^2}\right). \tag{17}$$

A previous study (Sale and Mathews 1986) considered a one parameter gaussian distribution with $\mu = 0$. Using this two parameter distribution we find

$$\bar{\eta} = \mu + \sqrt{\frac{2}{\pi}}\sigma\frac{e^{-\mu^2/2\sigma^2}}{1+\mathrm{erf}(\mu/\sqrt{2}\sigma.)}. \tag{18}$$

Note that this expression requires

$$\bar{\eta} \geq \sqrt{\frac{2}{\pi}}\sigma. \tag{19}$$

Thus a region of parameter space is already restricted by the mathematics. The results of the parameter space search are shown in figure 3. Using the weaker ^{7}Li bound (4) then $\bar{\eta}_{10} \lesssim 3.7$. If we include the WSSOK ^{7}Li bound then $\bar{\eta}_{10} \lesssim 3.4$. These results are summarized in table 1.

4.4 Power Law

We assume a featureless power law for the power spectrum (Peebles 1987a,b)

$$\langle|\delta_k|^2\rangle \propto k^n. \tag{20}$$

Thus $\Delta^2(k) \propto k^{n+3}$ and the average abundance (12) is

$$\bar{X}_i = \int_0^{\eta_{\max}} d\eta\,\eta f(\eta) X_i(\eta)\left[1-\left(\frac{\eta}{\eta_{\max}}\right)^{\frac{n+3}{2}}\right] \Bigg/ \int_0^{\eta_{\max}} d\eta\,\eta f(\eta)\left[1-\left(\frac{\eta}{\eta_{\max}}\right)^{\frac{n+3}{2}}\right]. \tag{21}$$

In the limit of $\eta_{\max} \to \infty$ ($k_{\max} \to \infty$) this reduces to the simpler case where the scale of the perturbations was ignored (6). Hence for $\eta_{\max} \gg \bar{\eta}$ we expect the results to be independent of the power law index, n. For each of the previously studied distribution functions we have performed the average as given above (21). The results are shown in figs. 4-6. The spectral index, $n = -0.5$ was chosen for illustrative purposes and since it is the preferred value in the PIB model.

As an example of the results with a power law distribution consider the gamma distribution (fig. 4). For $\delta^2 = 0.1$ (a) using the weaker ^{7}Li (4) there is a small band in the allowed parameter space between the ^{4}He and D + ^{3}He bounds. The WSSOK ^{7}Li value is only marginally consistent with the D + ^{3}He bound leaving a very narrow allowed region in parameter space. For $\delta^2 = 0.2$ (b) the limit from the weaker ^{7}Li value roughly overlays the ^{4}He limit and the WSSOK ^{7}Li value is inconsistent with the D + ^{3}He limit. For $\delta^2 = 0.5$ (c) ^{7}Li is always produced in greater amounts

than allowed according to the WSSOK limit. Finally for $\delta^2 = 1.0$ (d) ^{7}Li is always overproduced and the D + ^{3}He is inconsistent with the ^{4}He limit (there is no allowed parameter space).

From our expression for $\eta_c(k)$ (11), if $\eta_{\rm max} = 5 \times 10^{-10}$ then $\lambda_{\rm min} \approx 70$ kpc. Thus for this $\eta_{\rm max}$ the spectrum of perturbations must be cutoff at the (comoving) scale of 70 kpc. No structure on scales smaller than this could be created from baryon isocurvature baryon perturbations. To allow smaller scale structure to form we must lower $\lambda_{\rm min}$ and hence raise $\eta_{\rm max}$. Thus we use as our criteria for determining valid regions in parameter space that all the light element bounds are satisfied and $\eta_{\rm max} \gtrsim 5 \times 10^{-10}$. From fig. 4(a) we see that requiring structure on scales less than 70 kpc eliminates the horizontal region where the light element abundances are consistent with observations. From figs. 4(a-d), we see that this leads to a limit of $\bar{\eta}_{10} \lesssim 6.0$ with the weaker ^{7}Li abundance and $\bar{\eta}_{10} \lesssim 4.0$ for the WSSOK ^{7}Li bound. Similar results hold for the log normal (fig. 5) and gaussian (fig. 6) distributions. These results are also summarized in table 1. Notice, if we allow an arbitrary cutoff at $3.5 \times 10^{-10} \lesssim \eta_{\rm max} \lesssim 5 \times 10^{-10}$ we can get $\bar{\eta}$ to be as large as desired. However, this requires introducing new physics to explain the origin of the cutoff at 70–80 kpc.

We noted above that the results should be largely independent of the power law index, n. To verify this we have examined the gamma distribution for three values of n. The values chosen are $n = -0.5$ (fig. 4), $n = -2.5$ (fig. 7), and $n = 2.5$ (fig. 8). Comparing these figures we find that decreasing n slightly shifts the bounds to higher $\bar{\eta}$. This effect is most pronounced for $\delta^2 = 1.0$ (part (d) of the figures). However, since this effect is small and shift all bound in approximately the same manner, the limits quoted in table 1 are valid for all values of n.

5 Conclusions

As shown in table 1 the extra parameters used in these models of inhomogeneous BBN allow for only a slight increase in η over SBBN. This fact is easy to understand. First ignore the ^{7}Li limits. Since the abundance of ^{4}He is a monotonically increasing function of η and the abundances of D and ^{3}He are monotonically decreasing functions of η, when we include regions of high η we are overproducing (underproducing) ^{4}He (D and ^{3}He) in the universe. The slight increase in the allowed value for η comes from the fact that ^{4}He is a slowly varying function of η. When we include the ^{7}Li bound it provides the tight upper bound on η. This is due to the fact that the observed abundance lies in the trough of the predicted BBN production (see WSSOK). Thus any regions of high η greatly over produce ^{7}Li and we cannot allow such regions to have a significant contribution in the universe. The slight increase in η allowed is due to the generous limits we have allowed for the ^{7}Li abundance.

The case of a power law distribution allows only a slightly extended range at the expense of adding two new parameters, n and $\eta_{\rm max}$. The reason for this again traces back to the above discussion of mixing in regions with too much or too little of the light elements. Furthermore, these results are essentially independent of n. This in turn places tight constraints on models that contain these perturbations. In models that allow the power spectrum to extend to small scales the density of baryons is restricted to the same region as homogeneous BBN. Models that impose a small scale cutoff can, if the cutoff falls in just the right region, lead to much higher values for the baryon density at the expense of adding new physics. Recently Gnedin, Ostriker, & Rees (1994) have found some non-gaussian baryon isocurvature models can circumvent these bounds. We will return to this topic in a future work.

Acknowledgments

We would like to thank B. D. Fields, G. Gyuk, G. Mathews, M. S. Turner, P. J. E. Peebles, J. Ostriker, M. Rees, and E. Vishniac for useful conversations. During the final stages of manuscript preparation we became aware of a similar project by Jedamzik and Fuller (1994). Although we have not seen their manuscript we understand they reach similar conclusions. This work has been supported in part by NSF grant AST 90-22629, DOE grant DE-FG02-91-ER40606, and NASA grant NAGW-1321 at the University of Chicago, by the DOE and by NASA through grant NAGW-2381 at Fermilab, and the U. S. Department of Energy under contract DE-FG02-94ER-40823 at the University of Minnesota.

References

Barrow, J. D. and Morgan, J. 1983, *MNRAS* **203** 393.

Cen, R., Ostriker, J. P., and Peebles, P. J. E. 1993, *ApJ* **415** 423.

Copi, C. J., Schramm, D. N., and Turner, M. S. 1994, *Science* submitted.

Epstein, R. I. and Petrosian, V. 1975, *ApJ* **197** 281 (EP).

Gnedin, N. Y., Ostriker, J. P., and Rees, M. J. 1994, *ApJ* submitted.

Hogan, C. J. 1978, *MNRAS* **185** 889.

Hogan, C. J. 1993, *ApJ* **415** L63.

Izotov, Y. I., Thuan, T. X., and Lipovetsky, V. A. 1994, preprint.

Jedamzik, K. and Fuller, G. M. 1994, private communication.

Jedamzik, K., Fuller, G. M., and Mathews, G. J. 1994, *ApJ* **423** 50.

Kawano, L. H. 1992, FERMILAB-PUB-92/04-A, preprint.

Kernan, P. J. 1993, The Ohio State University, PhD thesis.

Kernan, P, J. & Krauss, L. M. 1994, *PRL* **72** 3309.

Kurki-Suonio, H., Matzner, R. A., Olive, K. A., & Schramm, D. N. 1990, *ApJ* **353** 406

Malaney, R. A. and Mathews, G. 1993, *Phys. Rep.* **229** 147.

Mathews, G. J., Meyer, B. S., Alcock, C. R., & Fuller, G. M. 1990, *ApJ* **358** 36.

Olive, K. A. and Steigman, G. 1994, UMN-TH-1230/94, preprint.

Pagel, B. J. E., Simonson, E. A., Terlevich, R. J., and Edmunds, M. G. 1992, *MNRAS* **255** 325.

Peebles, P. J. E. 1987a, *Nature* **327** 210.

Peebles, P. J. E. 1987b, *ApJ* **315** L73.

Rees, M. J. 1984, in *Formation and Evolution of Galaxies and Large Structures in the Universe*, eds., J. Audouze & J. Tran Thanh Van (Boston: D. Reidel Publishing Company), 271.

Sale, K. E. and Mathews, G. J. 1986, *ApJ* **309** L1.

Skillman E. D., Terlevich, R. J., Kennicut, R. C., Jr., Garnett, D. R., and Terlevich, E 1994a. *ApJ* **431** 172.

Skillman, E. D. *et al.* 1994b, *ApJL* in preparation.

Smith, M. S., Kawano, L. H., and Malaney, R. A. 1993, *ApJS* **85** 219.

Sato, K. & Terasawa, N. 1991, *Phys. Scr.* **T36**, 60

Thomas, D., Schramm, D. N., Olive, K. A., Mathews, G. J., Meyer, B. S. & Fields, B. D. 1994, *ApJ* **406** 569.

Thorburn, J. A. 1994, *ApJ* **421** 318.

Walker, T. P., Steigman, G., Schramm, D. N., Olive, K. A., and Kang, H. 1991, *ApJ* **376** 51 (WSSOK).

Yang, J., Turner, M. S., Steigman, G., Schramm, D. N., and Olive, K. A. 1984, *ApJ* **281** 493.

Figures

1. Parameter space plot for the gamma distribution. The acceptable parameter space is between the ^{4}He lines (solid), below and to the right of the D line (short-dash), above and to the right of the D + ^{3}He line (dash-dot), and below the WSSOK ^{7}Li line (long-dash) or below the Thorburn ^{7}Li line (long-dash, short-dash). The light gray shaded region satisfies the ^{4}He, D, D + ^{3}He, and Thorburn (weaker) ^{7}Li bounds. The dark gray shaded region satisfies the ^{4}He, D, D + ^{3}He, and WSSOK ^{7}Li bounds.

2. Parameter space plot for the log normal distribution. The acceptable parameter space is as defined in figure 1.

3. Parameter space plot for the gaussian distribution. The acceptable parameter space is as defined in figure 1. The region above the slanted solid line is not accessible for mathematical reasons (see text for details).

4. Parameter space plot for the gamma distribution with scale for $n = -1/2$. The acceptable parameter space is as defined in figure 1. In a) with $\delta^2 = 0.1$, $\bar{\eta} \lesssim 6 \times 10^{-10}$ for $\eta_{\rm max} \gtrsim 5 \times 10^{-10}$. In b) with $\delta^2 = 0.2$, the WSSOK ^{7}Li limit does not allow any region of concordance. In c) with $\delta^2 = 0.5$, the Thorburn ^{7}Li limit falls below the D + ^{3}He limit. In d) with $\delta^2 = 1.0$ ^{7}Li is overproduced for all values of $\bar{\eta}$ and $\eta_{\rm max}$ and the region defined by the D and D + ^{3}He limits does not overlap the region defined by the Y_P limits.

5. Parameter space plot for the log normal distribution with scale for $n = -1/2$. The acceptable parameter space is as defined in figure 1.

6. Parameter space plot for the gaussian distribution with scale for $n = -1/2$. The acceptable parameter space is as defined in figure 1.

7. Parameter space plot for the gamma distribution with scale for $n = -2.5$. The acceptable parameter space is as defined in figure 1.

8. Parameter space plot for the gamma distribution with scale for $n = 2.5$. The acceptable parameter space is as defined in figure 1.

Distribution Function	Upper limits on η_{10}	
	w/o WSSOK ^{7}Li	with WSSOK ^{7}Li
Gamma	3.6	3.3
Log normal	3.6	3.2
Gaussian	3.7	3.4
Power law + gamma	6.0	4.0
Power law + log normal	6.0	4.0
Power law + gaussian	5.0	4.0

Table 1: Upper limits on η_{10} for various distribution functions (see text for details).

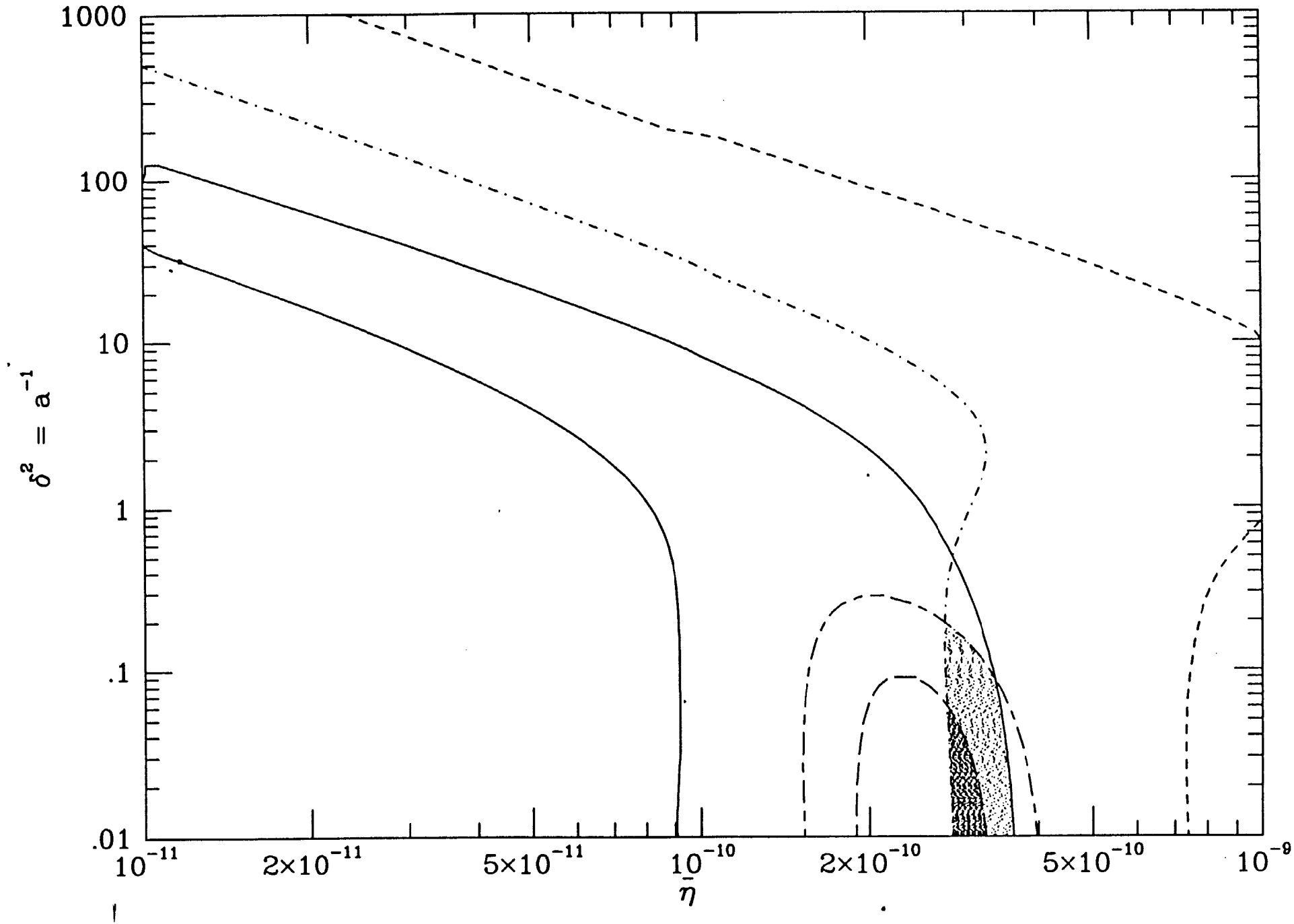
1000
100
10
1
.1
.01
$\delta^2 = a^{-1}$
10^{-11}
2×10^{-11}
5×10^{-11}
10^{-10}
2×10^{-10}
5×10^{-10}
10^{-9}
$\bar{\eta}$

fig 1

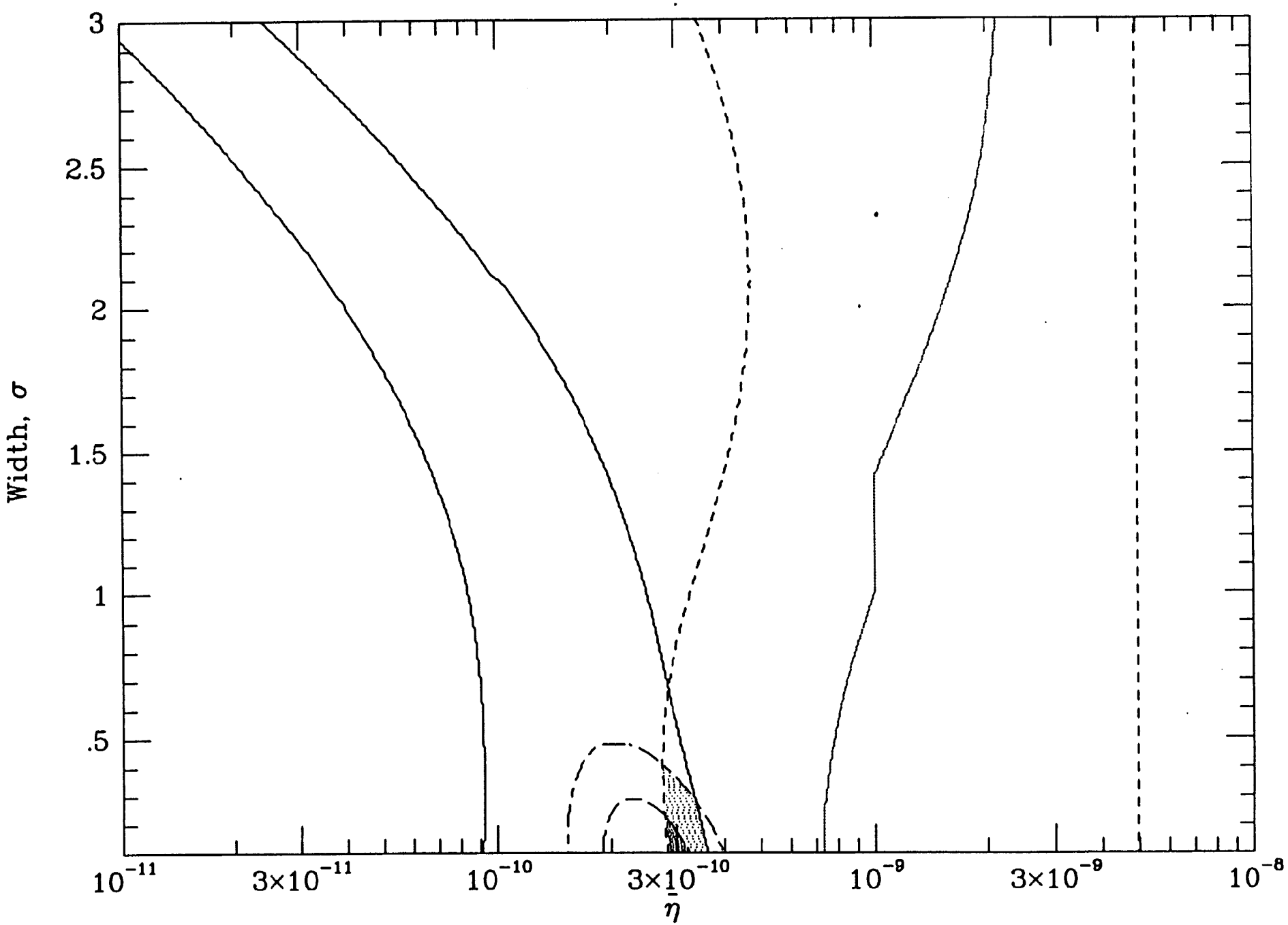

Fig 2

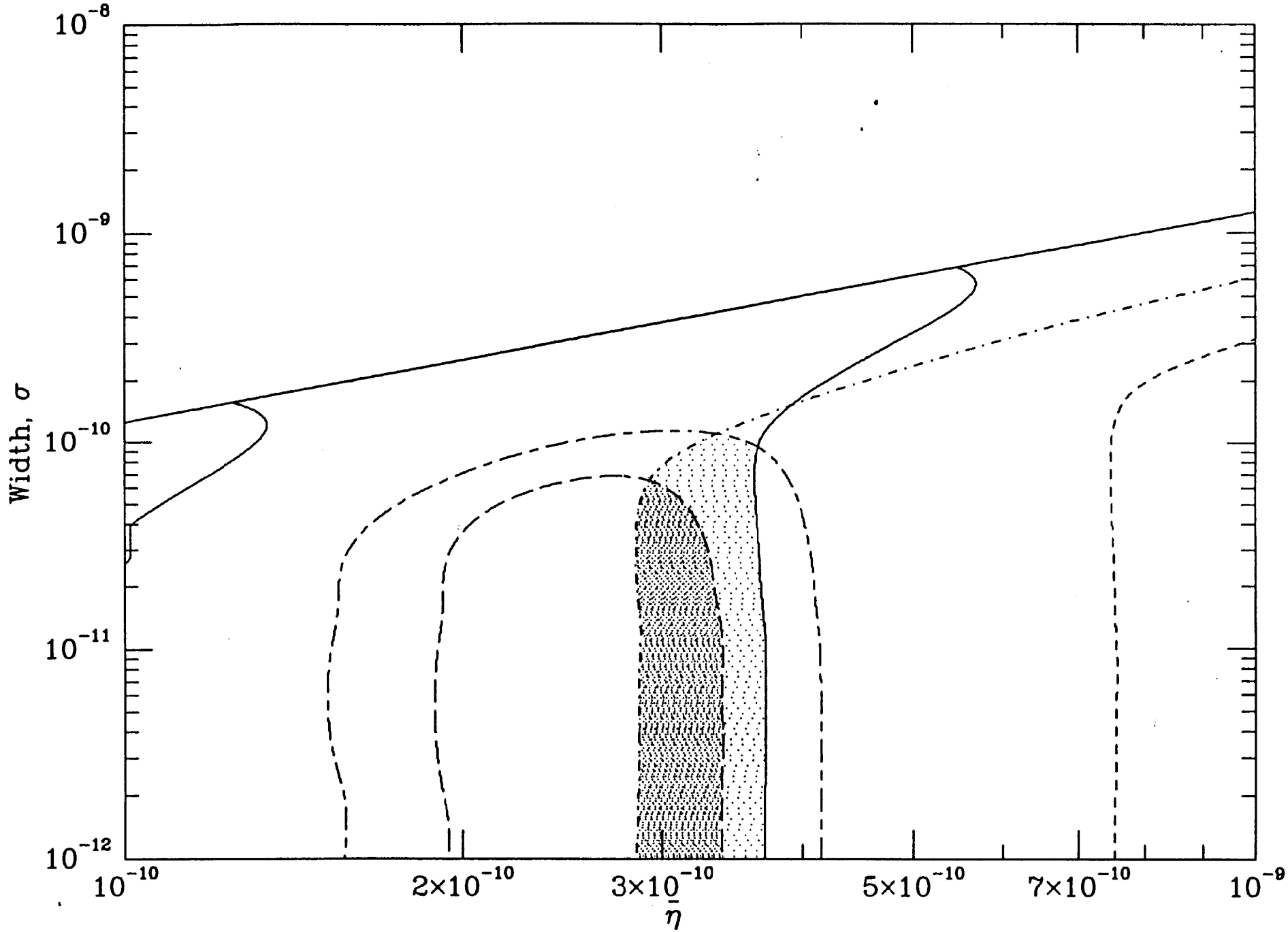
10^{-8}
10^{-9}
10^{-10}
10^{-11}
10^{-12}
Width, σ
10^{-10}
2×10^{-10}
3×10^{-10}
5×10^{-10}
7×10^{-10}
10^{-9}
$\bar{\eta}$

Fig 3

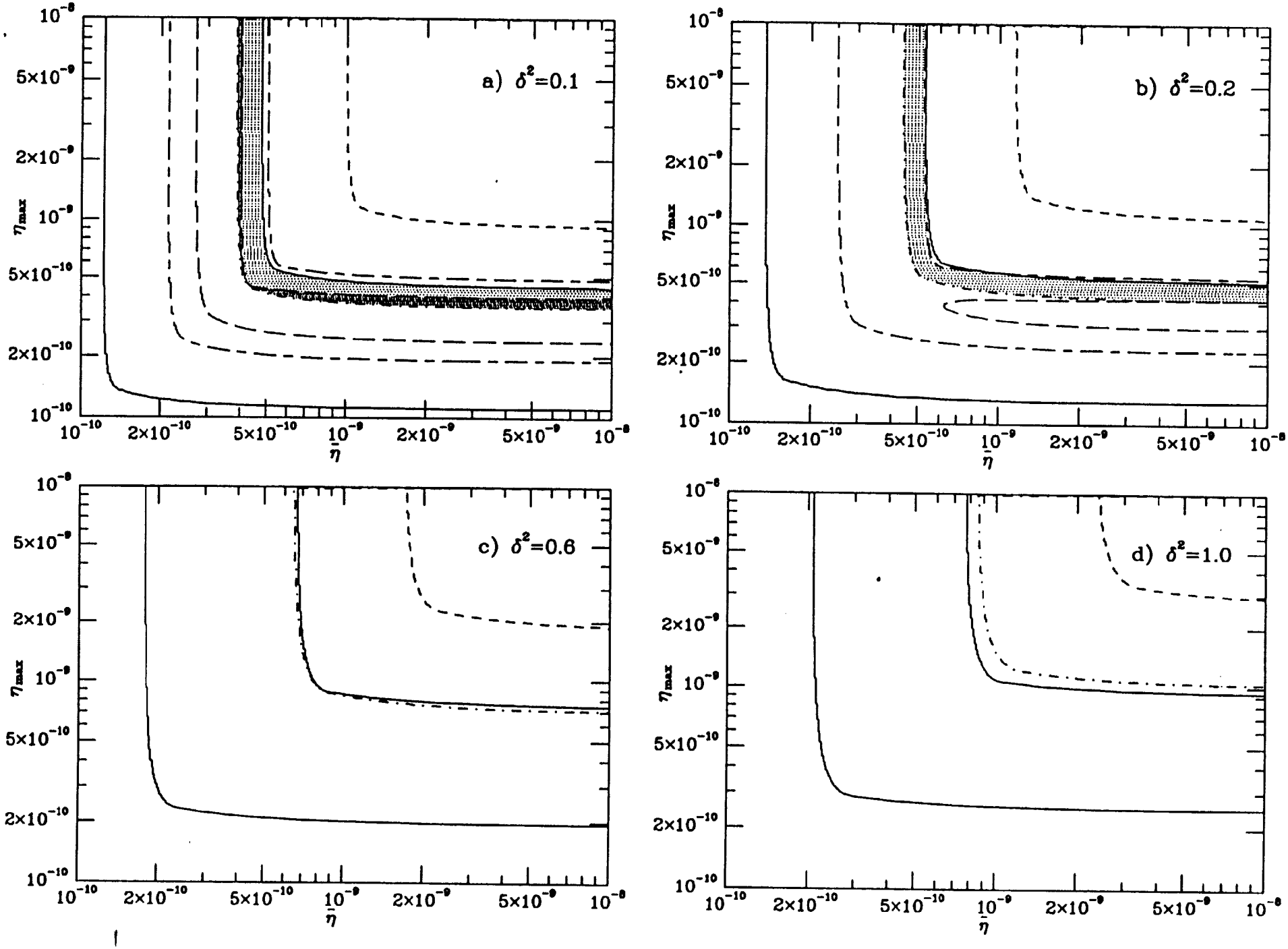
a) δ^2=0.1
b) δ^2=0.2
c) δ^2=0.6
d) δ^2=1.0
η_{max}
$\bar{\eta}$
10^{-8}
5×10^{-9}
2×10^{-9}
10^{-9}
5×10^{-10}
2×10^{-10}
10^{-10}

Fig 4

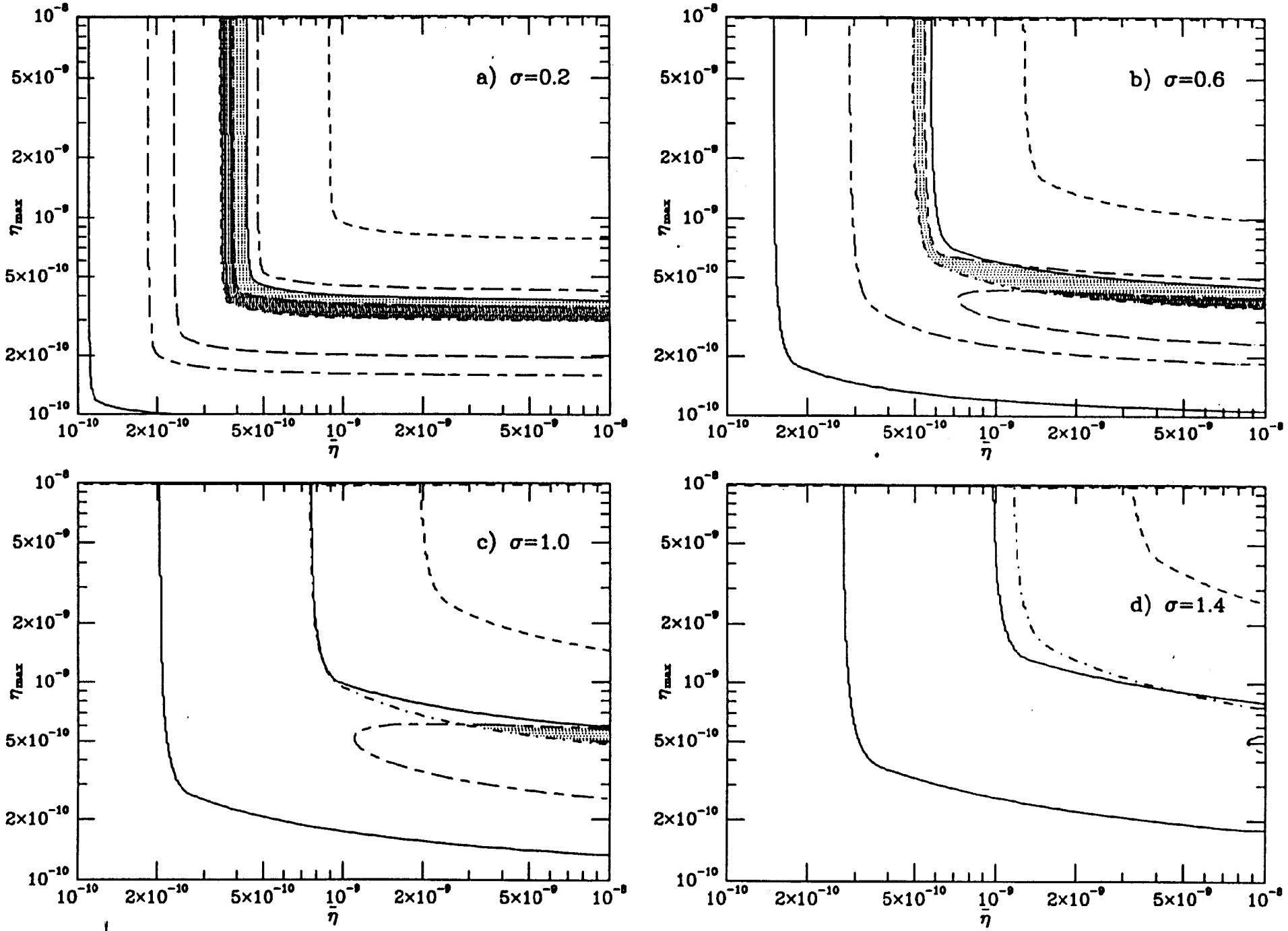
a) σ=0.2
b) σ=0.6
c) σ=1.0
d) σ=1.4
η_{max}
$\bar{\eta}$
10^{-8}
5×10^{-9}
2×10^{-9}
10^{-9}
5×10^{-10}
2×10^{-10}
10^{-10}

Fig 5

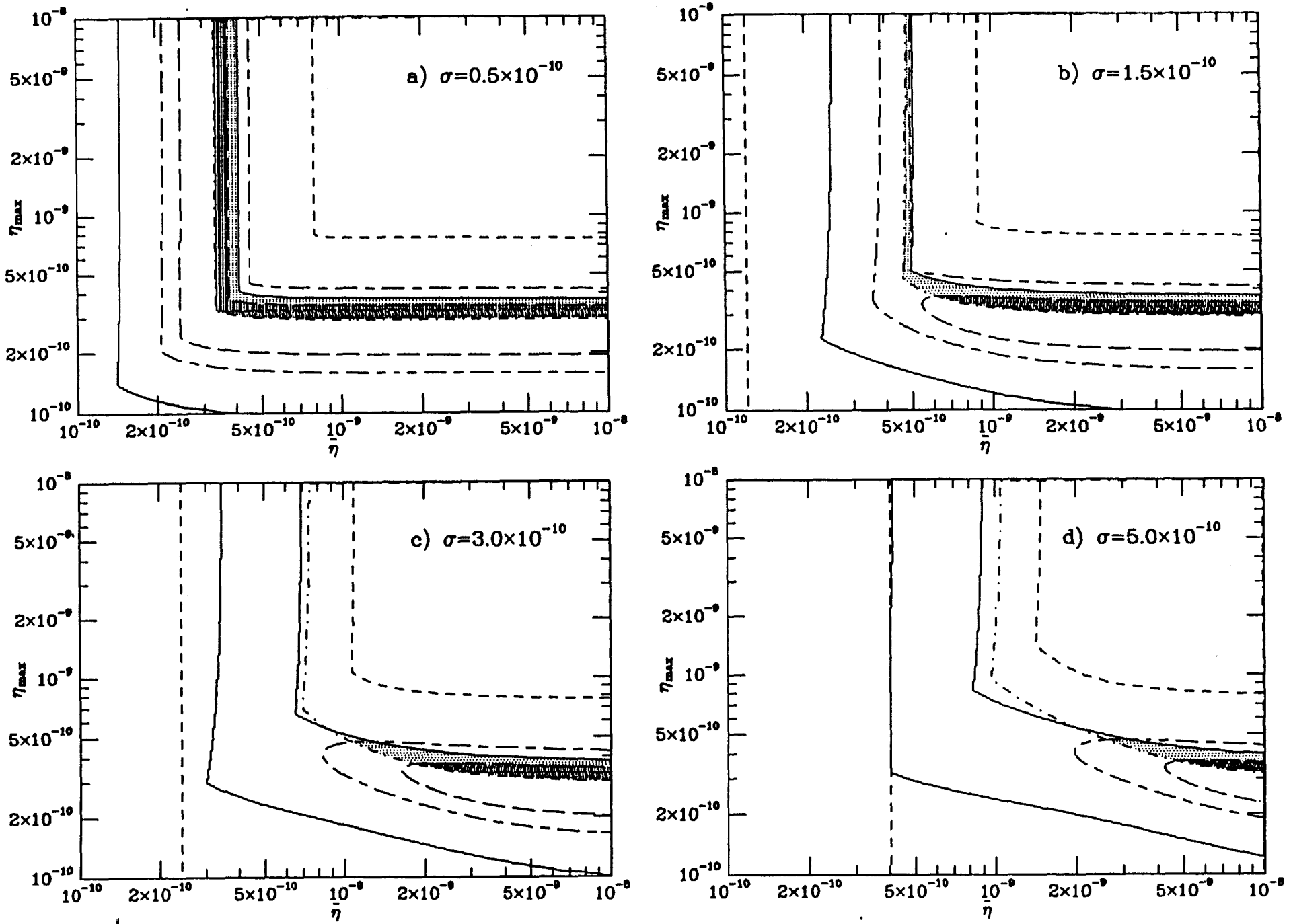
a) $\sigma=0.5\times10^{-10}$
b) $\sigma=1.5\times10^{-10}$
c) $\sigma=3.0\times10^{-10}$
d) $\sigma=5.0\times10^{-10}$
η_{max}
$\bar{\eta}$
10^{-8}
5×10^{-9}
2×10^{-9}
10^{-9}
5×10^{-10}
2×10^{-10}
10^{-10}

Fig 6

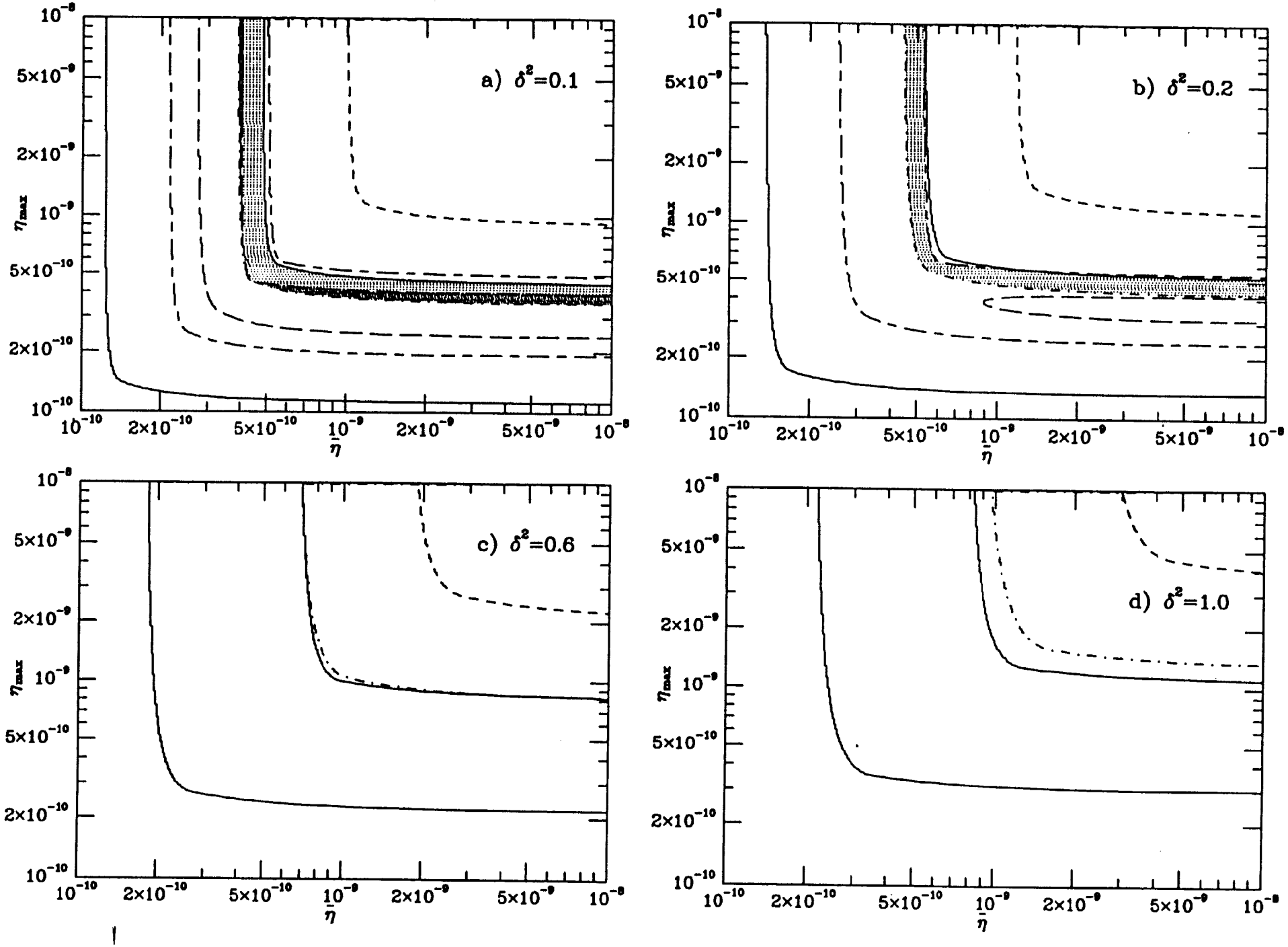
a) δ^2=0.1
b) δ^2=0.2
c) δ^2=0.6
d) δ^2=1.0
η_{max}
$\bar{\eta}$
10^{-8}
5×10^{-9}
2×10^{-9}
10^{-9}
5×10^{-10}
2×10^{-10}
10^{-10}

Fig 7

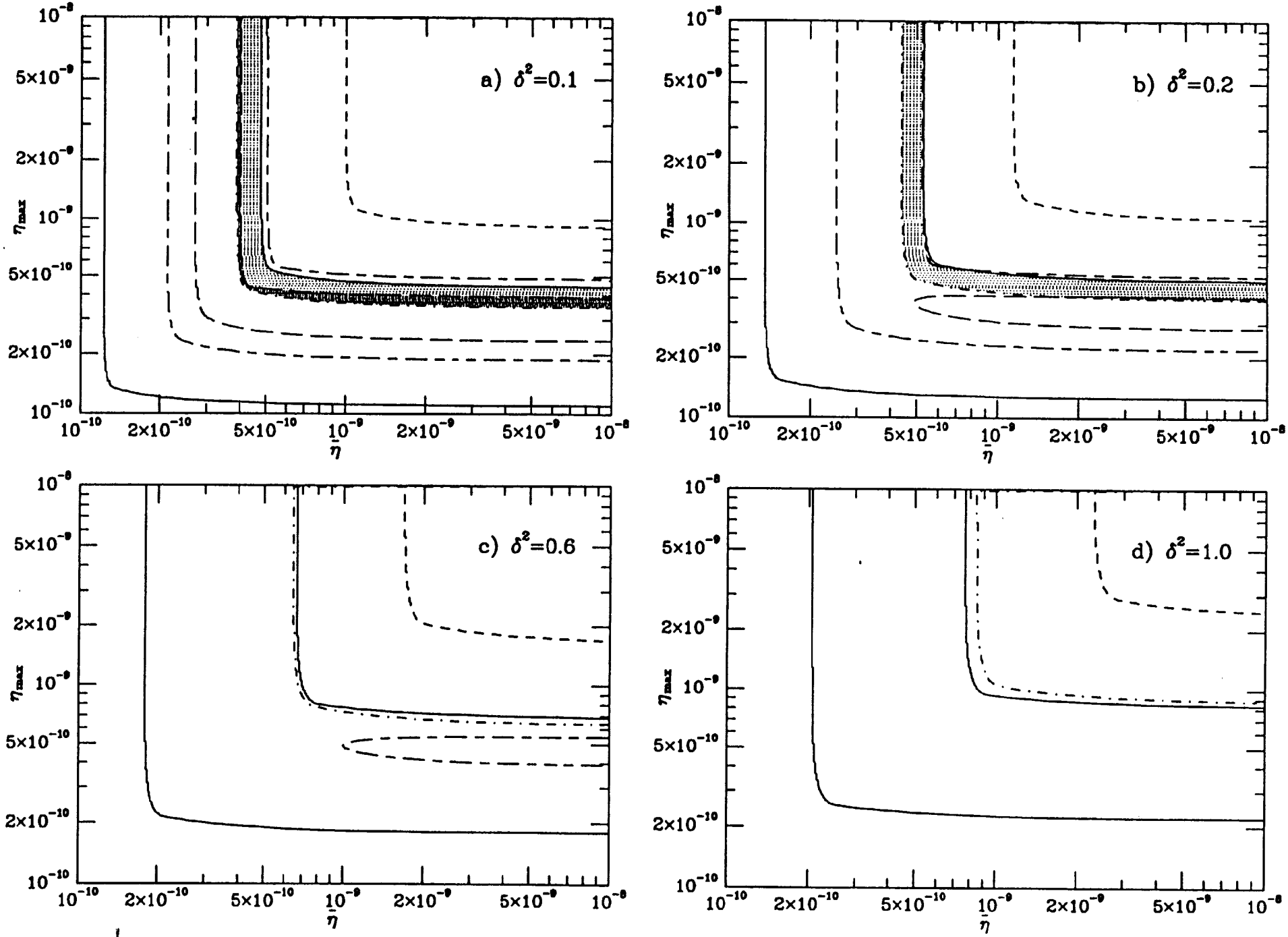
a) δ^2=0.1
b) δ^2=0.2
c) δ^2=0.6
d) δ^2=1.0
η_{max}
$\bar{\eta}$
10^{-8}
5×10^{-9}
2×10^{-9}
10^{-9}
5×10^{-10}
2×10^{-10}
10^{-10}

Fig 8